



## Research article

# Mechanisms of vemurafenib-induced anti-tumor effects in ATC FRO cells

Jingwei Xu <sup>a</sup>, Di Xue <sup>b</sup>, Yang Li <sup>b</sup>, Jianwen Zhou <sup>b</sup>, Hongyue Chen <sup>a</sup>, Li Fan <sup>b,\*</sup>

<sup>a</sup> Department of General Surgery, The First Affiliated Hospital of Qiqihar Medical University, Heilongjiang, 161041, China

<sup>b</sup> Research Institute of Medicine and Pharmacy of Qiqihar Medical University, Heilongjiang, 16006, China

## ARTICLE INFO

## Keywords:

Vemurafenib  
Anaplastic thyroid carcinoma  
BANCR  
PI3K/AKT pathway  
Proliferation and metastasis

## ABSTRACT

**Background:** Anaplastic Thyroid Carcinoma (ATC) is a rare and deadly malignant tumor in humans. It is prone to developing resistance to radiotherapy and chemotherapy. Molecular targeted therapy offers a novel way to treat ATC. The BRAF mutation is closely associated with many cancers, including thyroid carcinoma. Vemurafenib, a small-molecule inhibitor, is specifically designed to target the mutant serine/threonine kinase BRAF. The objective of this study is to elucidate the regulatory mechanisms underlying the effects of vemurafenib on human anaplastic thyroid carcinoma cell line FRO and to assess its potential therapeutic role.

**Methods:** The effects of vemurafenib on the proliferation of FRO cells were assessed by the CCK-8 method and Colony-forming assay. Transwell chambers and scratch tests were employed to examine the impact of vemurafenib on the invasion and migration of FRO cells. Apoptosis and cycle distribution of FRO cells were analyzed by tunel assay and flow cytometry. The effects of vemurafenib on the expression of BRAF-activated non-protein coding RNA (BANCR), Bax, Bcl2, and E-cadherin were evaluated by qRT-PCR. Furthermore, the effects of vemurafenib on the expression of phosphoinositol-3-kinase (PI3K)/phosphoinositol-3-kinase (AKT) pathway-related proteins, BRAF, CyclinD1, Bcl-2, Bax, and E-cadherin proteins in FRO cells were investigated through the western-blot method. All experiments were conducted in three replicates.

**Results:** Vemurafenib was observed to inhibit proliferation and induce apoptosis in a dose- and time-dependent manner ( $P < 0.05$ ). The formation of FRO cell colonies, as well as migration and invasion, all showed a dose-dependent reduction ( $P < 0.05$ ). Flow cytometric analysis indicated G0/G1 cell cycle arrest ( $P < 0.05$ ). QRT-PCR revealed that vemurafenib could suppress the expression of BANCR and Bcl2 while increasing the expression of Bax and E-cadherin in a dose-dependent manner ( $P < 0.05$ ). The protein expression levels of Bax and E-cadherin were up-regulated significantly, and the expression levels of BRAF, CyclinD1, Bcl-2, p-PI3K, p-AKT, and p-mTOR were markedly down-regulated with increasing concentrations of vemurafenib ( $P < 0.05$ ).

**Conclusions:** The proliferation and metastasis of FRO cells can be suppressed by vemurafenib through the silencing of BRAF and BANCR expression, inhibition of PI3K/AKT signaling pathway activation, induction of apoptosis, and cell cycle arrest.

\* Corresponding author.

E-mail address: [fan123456li@126.com](mailto:fan123456li@126.com) (L. Fan).

## 1. Introduction

Thyroid cancer is the most prevalent malignant tumor in the endocrine system. Anaplastic Thyroid Carcinoma (ATC) is a rare pathological type of thyroid carcinoma. Although the incidence rate of ATC is only 2%, it is one of the deadliest malignant tumors in humans, exhibiting extremely high malignancy, strong invasiveness, poor prognosis, susceptibility to radiotherapy, and chemotherapy resistance, with an average survival time of less than 6 months [1]. Currently, there is no effective treatment.

In recent years, within the context of precision medicine, specific gene mutations associated with different tumors have been identified, leading to the emergence of targeted therapies for these mutations. Molecular targeted therapy represents a novel approach to treating ATC. Research has shown that 90% of human malignant tumors have the BRAF mutation, and approximately 43–88% of papillary thyroid carcinoma and 20–40% of undifferentiated thyroid carcinoma have the BRAFV600E mutation [2,3]. The BRAF mutation is closely related to many cancers, including melanoma, non-small cell lung cancer, thyroid cancer, and colorectal cancer. It can dedifferentiate thyroid cancer cells, improve the recurrence rate, and reduce the survival rate [4]. The BRAF mutation mostly occurs at the 600th position, resulting from valine to glutamate (BRAFV600E), which leads to the constitutive activation of BRAF [5]. BRAF-activated non-protein coding RNA (BANCR) is a 693-base-long lncRNA that is situated on 9q21.11-q21.12 in a gene desert [6,7]. In recent years, it has been found that long-chain non-coding RNA (lncRNA) plays an important role in the occurrence and progression of various tumors. lncRNAs are about 200 nucleotides long and do not encode any proteins but regulate the expression of related genes [8]. BANCR is dysregulated in a variety of malignancies, affecting cell proliferation, migration, invasion, apoptosis, and epithelial-mesenchymal transition (EMT), and has become a potential target for tumor therapy [6]. Studies have shown that BANCR expression is elevated in thyroid tumor tissues compared to adjacent normal tissues. BANCR overexpression promotes migration and invasion of BCPAP cells by regulating the expression of E-cadherin, vimentin, and N-cadherin [9]. There was a strong correlation between the BRAFV600E mutation and BANCR expression and the tumor's size, bilateral location, multifocality, extracapsular invasion, and lateral lymph node metastases [10]. The precise mechanism of BANCR involvement in thyroid cancer is not entirely clear, but it is believed that BANCR may be involved in the signaling pathway of cancer occurrence.

Vemurafenib is a small molecule that effectively inhibits the mutant serine/threonine kinase BRAF. It selectively binds to the ATP binding site of the BRAF V600E kinase, inhibits its activity and cell proliferation only in BRAF mutant cell lines [11]. Matthias Lang et al. demonstrated that vemurafenib can improve the survival rate of melanoma patients, hairy-cell leukemia, and intracranial neoplasms with the BRAF V600E mutation [12]. Vemurafenib increases radioiodine uptake, up-regulates thyroid specific gene expression, and promotes tumor differentiation in a subset of patients with BRAF-mutant radioiodine-refractory thyroid cancer [13]. PI3K/AKT is one of the important signaling pathways of tumor metastasis, which is closely related to the mechanisms of tumor occurrence, metastasis, and drug resistance. Yalan Dai et al. elucidated that vemurafenib inhibits the immune escape biomarker BCL2A1 by targeting the PI3K/AKT signaling pathway to suppress breast cancer [14]. BINGNAN REN et al. showed that siBRAF inhibits the PI3K/AKT/mTOR signaling pathway synergistically, reducing biological activity while increasing chemosensitivity in non-small cell lung cancer (NSCLC) cells [15]. However, the precise effect of BRAF on the occurrence and development of ATC remains unknown. In this study, we examined the influence of vemurafenib on the proliferation and metastatic potential of anaplastic thyroid carcinoma FRO cells.

## 2. Materials and methods

### 2.1. Experimental reagents

Vemurafenib (Shanghai Biochempartner), Apoptosis Detection Kit (KeyGen BioTECH), Cell Cycle Assay Kit (Beyotime Biotechnology), primary antibodies and secondary antibodies (Proteintech), Fast Start Universal SYBR Green Master (ROX) (Roche), fetal bovine serum (FBS, Thermo Fisher). Microplate reader (Spark, Tecan), gel imager (ChemiDoc MP, Bio-Rad), quantitative polymerase chain reaction (qPCR) instrument (Q5, ABI), Flow Cytometry (Calibur, BD).

### 2.2. Cell culture

The Anaplastic thyroid cancer FRO cell line was purchased from the Cell Bank of the Chinese Academy of Sciences (Shanghai, China). The cells were cultured in RPMI 1640 medium supplemented with 10% FBS at 37 °C in a 5 % CO<sub>2</sub> incubator. Upon reaching 80% confluence, the cells were digested with 0.25% trypsin for sub-cultured or lyophilized for preservation.

### 2.3. CCK-8 assay for cell proliferation assessment

In the 96-well plate, 100 μL of logarithmic FRO cells (5 × 10<sup>4</sup> cells/mL) were added and cultivated at 37 °C with 5% CO<sub>2</sub>. When the cells were full to the bottom of the hole, the culture medium was sucked out. The final concentration (12.5, 25, 50, 100, and 200 μM) of the vemurafenib culture medium was added to continue the culture. The culture plates were removed after 24 and 48 h respectively. The culture medium was discarded, and cells were cultured in 100 μL of serum-free medium containing 10 μL of CCK-8 solution for 4 h. The absorbance (OD) of each well at 450 nm was measured by a microplate reader, and the inhibition rate of cell proliferation was calculated as [(control well A-experimental well A)/(control well A-blank well A) × 100%].

#### 2.4. Colony-forming assay

FRO cells in the logarithmic growth phase were digested by 0.25% trypsin and made into a single-cell suspension. Cell density was adjusted to 300 cells/mL. The cells were seeded in a 6-well cell culture plate at a concentration of 600 cells per well and then treated with different concentrations of vemurafenib (0, 12.5, 25, and 50  $\mu$ M) for 2–3 weeks. The medium was replaced at 3-day intervals. When the cell clones were observed, the cell culture solution was discarded. Cells were rinsed three times with PBS before being fixed for 15 min in 4% paraformaldehyde. Cells were stained with crystal violet staining (0.1%) for 20 min, followed by a gentle water wash and air drying. Finally, the clone formation rate was calculated as follows: (number of clones/number of inoculated cells)  $\times$  100%.

#### 2.5. Transwell chamber assay

FRO cells in the logarithmic growth phase were digested by 0.25% trypsin and transformed into a single-cell suspension. The cell density was adjusted to  $1 \times 10^6$  cells/mL using serum-free cell culture medium. A 100  $\mu$ L cell suspension containing vemurafenib (12.5, 25, and 50  $\mu$ M) was put into the upper chambers of the transwell chamber with and without Matrigel. The culture medium containing 10% FBS (700  $\mu$ L) was added into the lower chamber. The cells were incubated for 24 h at 37  $^{\circ}$ C with a 5% CO<sub>2</sub> incubator, after which the medium in the upper chamber was discarded and the cells in the upper chamber were washed twice with PBS, wiped clean with cotton swabs, fixed with 4% paraformaldehyde for 30 min, and dried. They were then stained with 0.1% crystal violet for 30 min and dried. Each sample was randomly selected from five views to photograph and count under a 200 $\times$  microscope. A similar methodology was used for migration detection, but transwell chambers were not coated with Matrigel.

#### 2.6. Wound healing experiment

FRO cells in the logarithmic growth phase were digested by 0.25% trypsin and prepared into a single-cell suspension. The cell density was adjusted to  $1 \times 10^6$  cells/mL. Each well was seeded with 2 mL in a 6-well plate and incubated at 37  $^{\circ}$ C in a 5% CO<sub>2</sub> chamber for 24 h. The bottom of the 6-well plate was scratched with a sterilized 20  $\mu$ L tip head. After washing with PBS three times, the cells were treated with varying concentrations of vemurafenib and incubated. After 0 h, 12 h, and 24 h, they were observed and photographed under a 200 $\times$  inverted microscope. The photomicrographs were then analyzed using Image J software.

#### 2.7. Cell cycle experiment by flow cytometry

FRO cells in the logarithmic growth phase were harvested and inoculated in a 6-well plate with a concentration of  $1 \times 10^6$  cells/mL, with 2 mL seeded into each well. The cells were treated with varying concentrations of vemurafenib and incubated for 24 h. The cells were collected and rinsed three times with precooled PBS before being made into a single cell suspension and dropwise added to precooled absolute ethanol until the final concentration was 70% before being fixed at 4  $^{\circ}$ C overnight. The fixed cells were rinsed with PBS twice, mixed with 400  $\mu$ L PI, and stained at 4  $^{\circ}$ C for 30 min, and the cell cycle was analyzed by flow cytometry.

#### 2.8. Flow cytometric analysis of cell apoptosis

FRO cells in the logarithmic growth phase were collected and inoculated in a 6-well plate with a concentration of  $1 \times 10^6$  cells/mL. Each well was seeded with 2 mL. The cells were treated with varying concentrations of vemurafenib and incubated for 24 h. The cells were collected, and the Annexin-V FITC Apoptosis Detection Kit was used as directed by the manufacturer. Apoptosis was subsequently quantified using flow cytometry.

#### 2.9. Detection of apoptosis using the TUNEL assay

FRO cells in the logarithmic growth phase were collected and inoculated in a 6-well plate with a concentration of  $1 \times 10^6$  cells/mL. Each well was seeded with 2 mL. The cells were treated with varying concentrations of vemurafenib and incubated for 24 h. Cells were fixed with 4% methanol solution at room temperature for 1 h and treated with 0.1% Triton X-100 for 2 min. Apoptotic staining was performed according to the instructions of the TUNEL apoptosis detection kit, and the TUNEL staining results were observed by confocal microscope. Six high-power fields were randomly selected to calculate the proportion of apoptotic cells in tumor cells, which was the apoptotic index.

**Table 1**  
Primer information in RT-PCR.

Genes	Upstream primer (5'-3')	Downstream primer (5'-3')
BANCR	CCTTCTGTAGGGTCTGGATTG	CATTGGTGCTGCAGTCTATTTC
Bax	TGGCTGGGGAGACACCTGAGC	TCAGCCCATCTTCTCCAGATG
Bcl-2	CATGTGTGTGAGAGCGTCA	CACTTGTGGCTCAGATAGGCA
E-cadherin	CTGAGAACGAGGCTAACG	GTCCACCATCATCATCAATAT
GAPDH	GGAGCGAGATCCCTCCAAAT	GGCTGTTGCATACCTCTCATGG

### 2.10. Quantitative real-time PCR (qRT-PCR)

FRO cells in the logarithmic growth phase were collected and inoculated in a 6-well plate with a concentration of  $1 \times 10^6$  cells/mL. Each well was seeded with 2 mL. The cells were treated with varying concentrations of vemurafenib and incubated for 24 h. Total RNA extraction, the cDNA synthesis procedure, and the PCR reaction were performed in accordance with the manufacturer's instructions.  $2^{-\Delta\Delta Ct}$  was used for relative quantitative analysis. Table 1 provides the quantitative primer information.

### 2.11. Western blot

FRO cells were treated and grouped as described in the previous experiment. Total proteins were extracted using a RIPA lysis buffer and quantified by the BCA method. SDS-PAGE electrophoresis was carried out for protein separation. The proteins were transferred to a PVDF membrane, which was blocked overnight with 5% skim milk powder at 4 °C. Subsequently, the membrane was incubated with antibodies and visualized by a gel imaging system. The expression of various proteins was detected, including p-PI3K, p-AKT, p-mTOR, PI3K, AKT, mTOR, Bax, Bcl-2, and E-cadherin.

### 2.12. Statistical analysis

SPSS 19.0 software was employed for comprehensive data analysis, and the measurement data were presented as mean  $\pm$  SD. One-way ANOVA was utilized for comparing multiple groups, while a *t*-test was used for two-way comparisons. Values of  $p < 0.05$  were considered statistically significant. The bar graph was plotted using GraphPad Prism 7.0.

## 3. Results

### 3.1. Vemurafenib exerts potent dose- and time-dependent inhibition on FRO cell proliferation

FRO cells were treated with various concentrations of vemurafenib for 24 and 48 h, as demonstrated by the results of the CCK-8 experiment (Fig. 1A), which showed that vemurafenib significantly inhibited the proliferation of FRO cells in a time- and dose-dependent manner. The IC<sub>50</sub> value for FRO cells treated with vemurafenib for 24 and 48 h was 32.13  $\mu$ M and 17.61  $\mu$ M, respectively. Consequently, cells treated with 12.5  $\mu$ M, 25  $\mu$ M, and 50  $\mu$ M of vemurafenib for 24 h were selected for subsequent experiments. Vemurafenib also significantly suppressed the clonal formation of FRO cells (Fig. 1B).

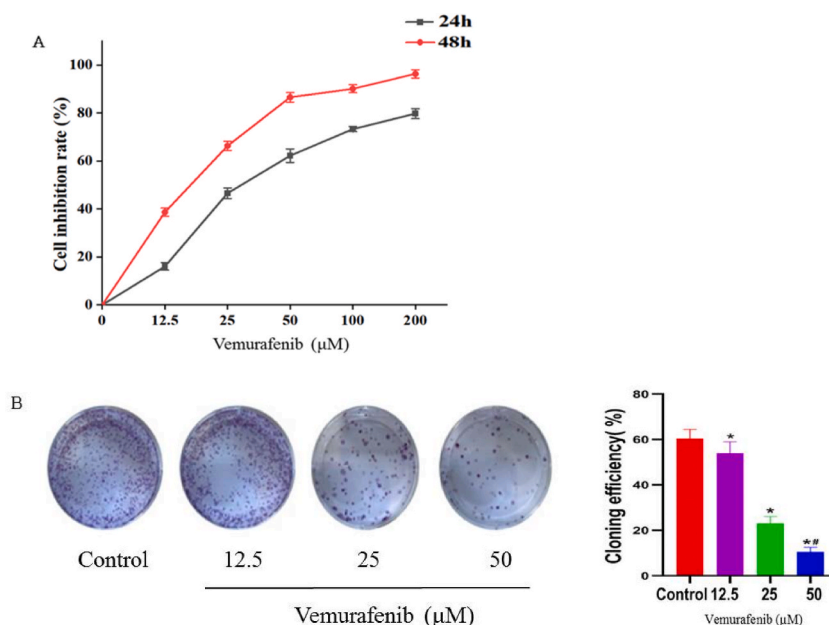


**Fig. 1.** Vemurafenib inhibited the viability of FRO cells.

(A) FRO cells were treated with the indicated concentrations of vemurafenib for 24 and 48 h, followed by CCK-8 assay for cell proliferation capacity. The data are shown as mean  $\pm$  SD,  $n = 3$ . (B) The clonal formation rate was measured by the colony survival test after FRO cells were treated with the indicated concentrations of vemurafenib for 24 h. The data are shown as the means  $\pm$  SD,  $n = 3$ . \* $P < 0.05$  compared with the control group; \*\* $P < 0.05$  compared with the 12.5  $\mu$ M group.

### 3.2. Vemurafenib significantly inhibited the invasion and migration of FRO cells

The transwell chamber assay demonstrated that vemurafenib inhibited FRO cell invasion and migration by decreasing the number of traversed cells in a concentration-dependent manner (Fig. 2A and B). Scratch healing experiments demonstrated that vemurafenib remarkably depressed the scratch healing rate of FRO cells compared to the control group (Fig. 2C). Furthermore, Western blot and qRT-PCR analyses were performed to assess the expression of molecules associated with invasion and migration markers. Our findings indicate that vemurafenib can up-regulate E-cadherin in a concentration-dependent manner (Figs. 5 and 6B).

### 3.3. Vemurafenib-induced cell cycle arrest in FRO cells

Different cell cycle phases of FRO cells were analyzed through flow cytometry. Results (Fig. 3) showed that the G0/G1 phase cells were observed to increase with the increase in vemurafenib concentrations. This indicated that the cell cycle had been arrested at the G0/G1 phase. Compared with the control group, the dosing group increased significantly (Table 2). We also assessed the expression of regulatory molecules connected to the G0/G1 phase concerning cell cycle markers. The discovery was that vemurafenib could down-regulate CyclinD1 in a concentration-dependent manner (Fig. 6B).

Flow cytometric analysis of the effects of vemurafenib on the FRO cell cycle. Results showed the percentage of cells in the G0/G1, S, and G2/M phases. G0/G1 phase cells increased remarkably with increasing vemurafenib concentrations.

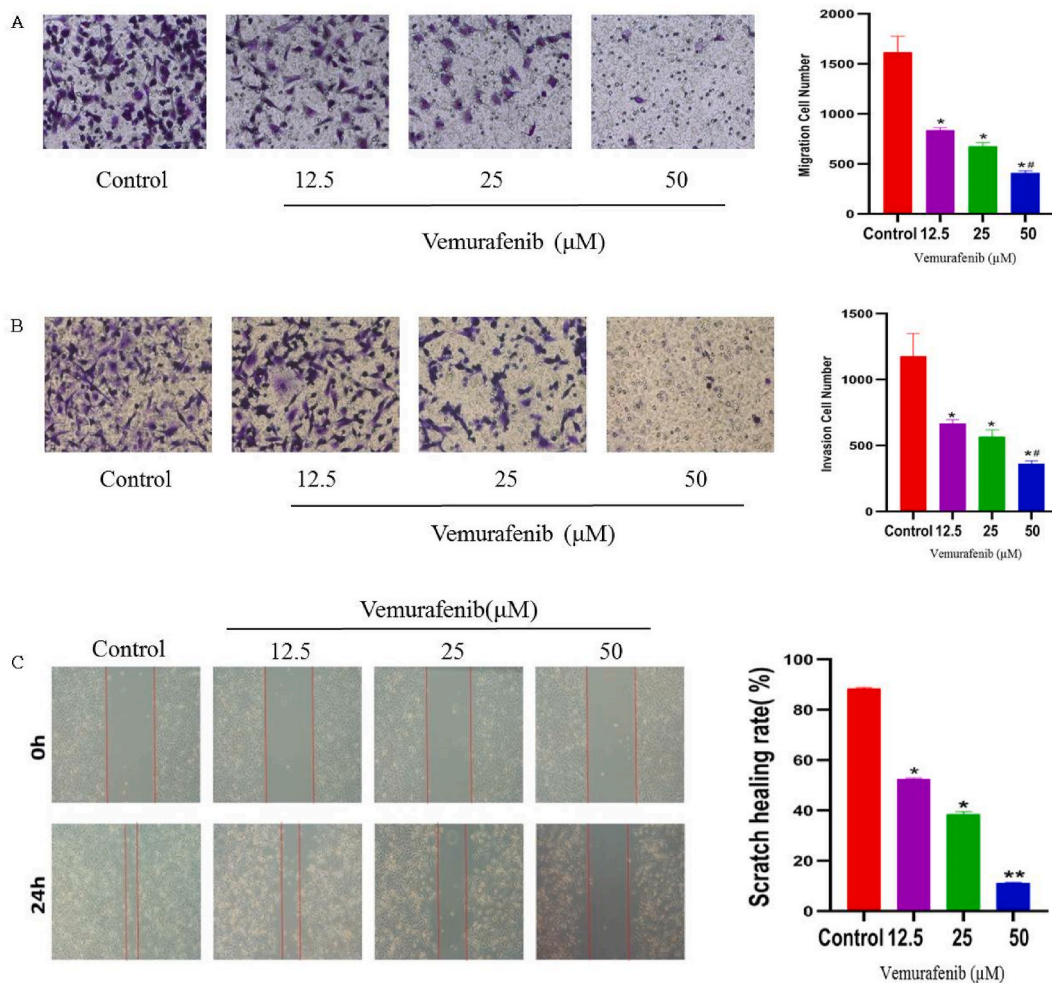


**Fig. 2.** Vemurafenib inhibited the invasion and migration of FRO cells. (A) The migration and (B) invasion of FRO cells were assessed using the transwell assay. (C) The healing ability of FRO cells was detected by a cell scratch assay. \* $P < 0.05$ ; \*\* $P < 0.01$  compared with the control group; # $P < 0.05$  compared with the 12.5 μM group.

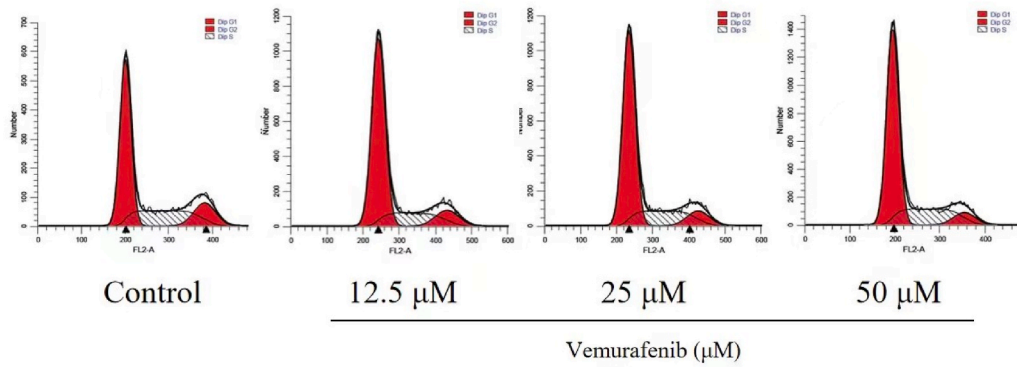


**Fig. 3.** Vemurafenib induced G0/G1 arrest in FRO cells.

**Table 2**  
Effects of vemurafenib on FRO cell cycle distribution (mean ± SD, n = 3).

Group	Cell cycle rate (%)		
	G0/G1	S	G2/M
Control	55.93 ± 0.53	15.51 ± 0.68	28.56 ± 0.67
12.5 μM	64.41 ± 0.86*	10.63 ± 1.06	24.96 ± 1.15
25 μM	68.23 ± 1.07*	9.35 ± 1.21	22.42 ± 1.12
50 μM	72.61 ± 0.92*	7.59 ± 0.78	19.80 ± 1.34

Note: \*P < 0.05 compared with the control group.

**3.4. Vemurafenib-induced apoptosis in FRO cells through the mitochondrial apoptotic pathway**

An annexin V/PI staining test was used to evaluate apoptosis through flow cytometry. Results showed that the rates of early and late apoptosis markedly increased as the concentration of vemurafenib increased. This indicated that vemurafenib promotes FRO cell apoptosis in a dose-dependent manner. (Fig. 4A). The TUNEL kit detects nuclear DNA breaks during apoptosis by labeling the broken

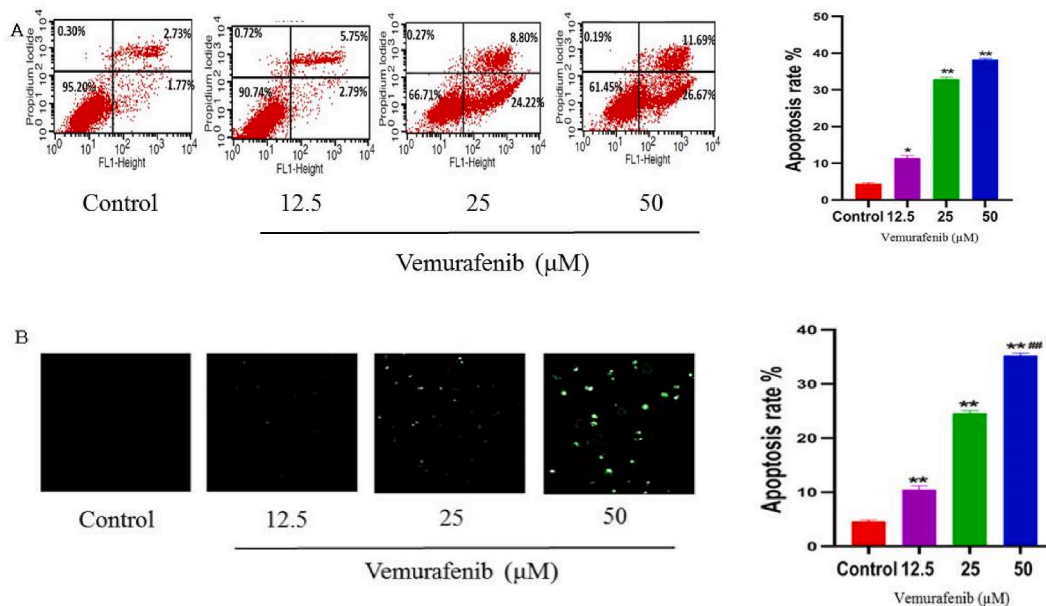


**Fig. 4.** Vemurafenib induced apoptosis of FRO cells (A) Annexin V-FITC/PI double labeling was used to quantify apoptotic rates by flow cytometry. (B) Cells stained with TUNEL and viewed under a laser scanning confocal microscope show apoptosis. \*P < 0.05, \*\*P < 0.01 compared with the control group; ##P < 0.01 compared with the 12.5 μM group.

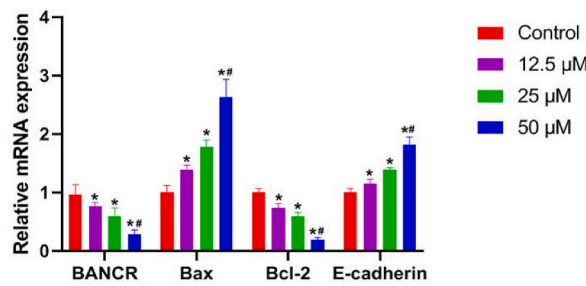


**Fig. 5.** Effect of vemurafenib on the associated mRNA expressions in FRO cells (mean ± SD, n = 5) QRT-PCR results showed that vemurafenib raised the mRNA expression of *Bax* and *E-cadherin* while decreasing *Bcl-2* and *BANCR* in a concentration-dependent manner. \* $P < 0.05$  compared with the control group; # $P < 0.01$  compared with the 12.5 μM group.

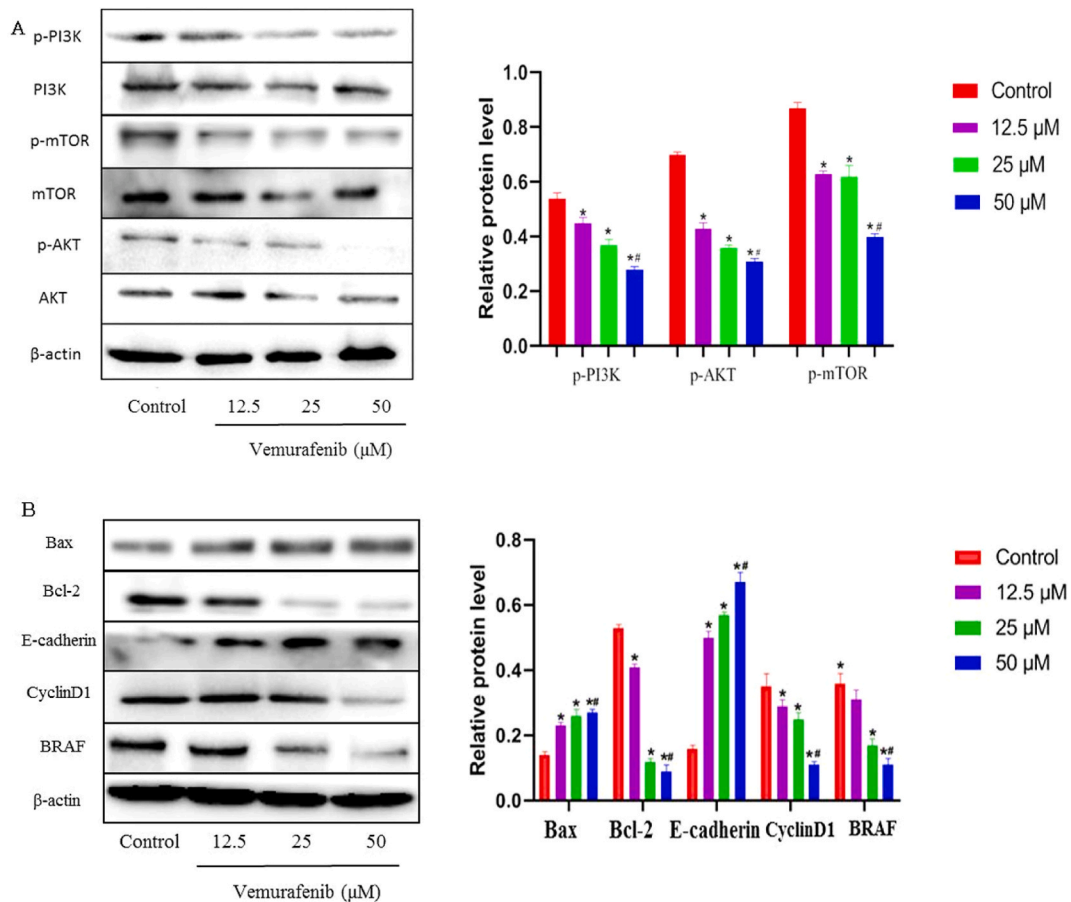


**Fig. 6.** Western-blot analysis of vemurafenib on the expression of related proteins in FRO cells (A) Vemurafenib decreased p-mTOR, p-AKT, and p-PI3K levels. (B) Vemurafenib decreased Bcl-2, CyclinD1, and BRAF levels, increased Bax and E-cadherin levels. \* $P < 0.05$  compared with the control group; # $P < 0.05$  compared with the 12.5 μM group.  $\beta$ -actin was employed as a normalization control.

DNA with green fluorescence. The results showed that the number of apoptotic cells increased significantly with increasing vemurafenib concentration (Fig. 4B). We checked the expression of regulatory molecules associated with the mitochondrial apoptosis pathway by Western blot and qRT-PCR. Results showed that Bcl-2 decreased significantly with increasing vemurafenib concentrations. The opposite was true for Bax (Figs. 5 and 6B).

### 3.5. Vemurafenib inhibited the target protein BRAF and its downstream LncRNA BANCR expression

The results showed that the expressions of *BANCR* and *BRAF* decreased significantly compared with the control (Figs. 5 and 6B).

### 3.6. The effect of vemurafenib on the PI3K/AKT pathway by western blot

The effect of vemurafenib on the expression of PI3K/AKT pathway-related proteins was assessed by Western blot. The results indicated that PI3K, AKT, and mTOR expression levels did not exhibit significant differences between groups. However, compared with the control group, the levels of p-PI3K, p-AKT, and p-mTOR decreased significantly with increasing concentrations of vemurafenib (Fig. 6A).

## 4. Discussion

According to the Joint Cancer Committee of the United States, patients with ATC are classified as having stage IV tumors from the onset of cancer [16]. Traditional treatments such as routine surgery, radiotherapy, and chemotherapy are ineffective, and the median survival time is only 5 months [17]. Targeted therapy is a new anti-tumor direction that has been developed in recent years. Therefore, it is crucial to search for effective targeted inhibitors for the treatment of thyroid cancer. Vemurafenib is a novel small-molecule BRAF inhibitor that has been approved by the US Food and Drug Administration for the treatment of patients with melanoma [18]. It has demonstrated promising results in the treatment of numerous BRAF mutant tumors [19]. In this study, we found that vemurafenib could inhibit the proliferation, invasion, and migration of FRO cells. It also induced cell apoptosis and promoted cell cycle arrest at the G0/G1 phase.

Malignant tumor cells have the biological characteristic of unlimited proliferation [20]. Vemurafenib was found to inhibit the activity and colony formation of FRO cells. The results showed that vemurafenib can interfere with cell proliferation. Cell cycle progression determines cell proliferation capacity. We observed that vemurafenib arrested the cell cycle in the G0/G1 phase of FRO cells. Different cyclin proteins are expressed in different phases of the cell cycle. Cyclin D1 is a typical marker of the G0/G1 phase and plays an important role in regulating the G0/G1 phase [21]. We found that vemurafenib downregulated cyclin D1 protein levels. The above results indicate that vemurafenib inhibits cell proliferation by inducing G0/G1 phase arrest in thyroid cancer cells.

DNA is the carrier of almost all biological genetic information. Many anticancer drugs induce DNA damage, which can lead to apoptosis [22]. Therefore, we examined the level of apoptosis in FRO cells treated with vemurafenib by tunel analysis. The results showed that vemurafenib induced DNA damage and promoted apoptosis in FRO cells, and flow cytometry results further indicated that vemurafenib promoted apoptosis in FRO cells. We proceeded to investigate the mechanism of vemurafenib-induced apoptosis. PI3K/AKT/mTOR is a classical signaling pathway that regulates cell proliferation, migration, invasion, and apoptosis [23–26] as well as a series of downstream substrates, among which the Bcl-2 family plays a crucial role in the mitochondrial apoptosis pathway. The anti-apoptotic protein BCL-2 binds to mitochondria and prevents the release of cytochrome *c* from mitochondria into the cytoplasm. In contrast, the pro-apoptotic protein BAX translocalizes to mitochondria and increases mitochondrial membrane permeability, thereby initiating apoptosis [27–31]. Inhibition of the PI3K/AKT/mTOR signaling pathway and promotion of E-cadherin expression can inhibit the proliferation and invasion of pancreatic cancer cells [32]. The results showed that vemurafenib significantly inhibited the activity of the PI3K/AKT/mTOR pathway, down-regulated the expression of BCL-2 protein, and up-regulated the expression of BAX protein and E-cadherin protein.

Several studies have explored the role of BRAF-activated non-protein coding RNA (*BANCR*) in cancer biology [33]. *BANCR* can act as a stem cell regulator in papillary thyroid cancer, enhancing cancer cell migration and invasion via the RAF/MEK/ERK signaling pathway [34]. It was shown that the expression of *BANCR* was upregulated in OSCC tissues and cell lines. *BANCR* may play an important role in OSCC development, cell proliferation, migration, and invasion. The results also showed that the expression of MAPK and PI3K/AKT pathway-related proteins p-ERK and p-AKT was positively correlated with the expression of *BANCR* [35]. In this study, we found that vemurafenib significantly inhibited the expressions of *BRAF* and *BANCR*, which were drug-dose-dependent. p-PI3K and p-AKT were positively correlated with the expressions of *BRAF* and *BANCR*. To sum up, vemurafenib can inhibit the expression of *BRAF* and *BANCR* and the activation of the PI3K/AKT/mTOR pathway, regulate the downstream expression of Bcl-2/Bax, up-regulated E-cadherin protein, induce apoptosis, inhibit cell proliferation, and reduce cell metastasis. Therefore, as a BRAFV600E-targeting inhibitor, vemurafenib may provide a future direction for the treatment of ATC containing BRAFV600E.

However, our study also has limitations. For instance, the current study was a single-cell experiment, and further animal experiments could improve the reliability of the findings.

### Ethics declarations

Informed consent was not required for this study.

### Consent for publication

Consent for publication was obtained from the participants.

## Funding

This study was supported by: Clinical Research Fund Project-Qiqihar Institute of Medical Sciences (No. QMSI2019-05); Scientific Research Topics of Heilongjiang Provincial Health and Wellness Commission (No.2021040401350).

## Data availability statement

Data will be made available on request.

## CRediT authorship contribution statement

**Jingwei Xu:** Writing – review & editing, Writing – original draft, Resources, Methodology, Investigation, Formal analysis, Data curation, Conceptualization. **Di Xue:** Writing – review & editing, Writing – original draft, Resources, Methodology, Investigation, Formal analysis, Data curation, Conceptualization. **Yang Li:** Methodology. **Jianwen Zhou:** Investigation. **Hongyue Chen:** Data curation. **Li Fan:** Writing – review & editing, Writing – original draft, Visualization, Supervision, Resources, Project administration, Methodology, Investigation, Funding acquisition, Data curation.

## Declaration of competing interest

The authors declare that they have no known competing financial interests or personal relationships that could have appeared to influence the work reported in this paper.

## Appendix A. Supplementary data

Supplementary data to this article can be found online at <https://doi.org/10.1016/j.heliyon.2024.e27629>.

## References

- [1] C. Jungels, J.M. Pita, G. Costante, Anaplastic thyroid carcinoma: advances in molecular profiling and targeted therapy, *Curr. Opin. Oncol.* 35 (1) (2023 Jan 1) 1–9, <https://doi.org/10.1097/CCO.0000000000000918>.
- [2] R.S. Scheffel, J.M. Dora, A.L. Maia, BRAF mutations in thyroid cancer, *Curr. Opin. Oncol.* 34 (1) (2022 Jan 1) 9–18, <https://doi.org/10.1097/CCO.0000000000000797>.
- [3] Y. Lu, X. Guo, M. Yang, K. Wang, G. Cao, Y. Liu, X. Hou, L. Chen, K. Liang, BRAFV600E genetic testing should be recommended for Bethesda III or V thyroid nodules based on fine-needle aspiration, *Sci. Rep.* 13 (1) (2023 Oct 10) 17129, <https://doi.org/10.1038/s41598-023-44464-1>.
- [4] J.M. Oh, B.C. Ahn, Molecular mechanisms of radioactive iodine refractoriness in differentiated thyroid cancer: impaired sodium iodide symporter (NIS) expression owing to altered signaling pathway activity and intracellular localization of NIS, *Theranostics* 11 (13) (2021 Apr 15) 6251–6277, <https://doi.org/10.7150/tno.57689>.
- [5] Y. Gao, D. Zhang, F. Wang, D. Zhang, P. Li, K. Wang, BRAF V600E protect from cell death via inhibition of the mitochondrial permeability transition in papillary and anaplastic thyroid cancers, *J. Cell Mol. Med.* 26 (14) (2022 Jul) 4048–4060, <https://doi.org/10.1111/jcmm.17443>.
- [6] B.M. Hussen, T. Azimi, A. Abak, H.J. Hidayat, M. Taheri, S. Ghafouri-Fard, Role of lncRNA BANCR in human cancers: an updated review, *Front. Cell Dev. Biol.* 9 (2021 Aug 2) 689992, <https://doi.org/10.3389/fcell.2021.689992>.
- [7] R.J. Flockhart, D.E. Webster, K. Qu, N. Mascarenhas, J. Kovalski, M. Kretz, P.A. Khavari, BRAFV600E remodels the melanocyte transcriptome and induces BANCR to regulate melanoma cell migration, *Genome Res.* 22 (6) (2012 Jun) 1006–1014.
- [8] M.C. Jiang, J.J. Ni, W.Y. Cui, B.Y. Wang, W. Zhuo, Emerging roles of lncRNA in cancer and therapeutic opportunities, *Am. J. Cancer Res.* 9 (7) (2019 Jul 1) 1354–1366. PMID: 31392074; PMCID: PMC6682721.
- [9] Y. Wang, J. Gu, X. Lin, W. Yan, W. Yang, G. Wu, lncRNA BANCR promotes EMT in PTC via the Raf/MEK/ERK signaling pathway, *Oncol. Lett.* 15 (4) (2018 Apr) 5865–5870, <https://doi.org/10.3892/ol.2018.8017>.
- [10] C. Shi, J. Cao, T. Shi, M. Liang, C. Ding, Y. Lv, W. Zhang, C. Li, W. Gao, G. Wu, J. Man, BRAFV600E mutation, BRAF-activated long non-coding RNA and miR-9 expression in papillary thyroid carcinoma, and their association with clinicopathological features, *World J. Surg. Oncol.* 18 (1) (2020 Jun 27) 145, <https://doi.org/10.1186/s12957-020-01923-7>.
- [11] I. Proietti, N. Skroza, S. Michelini, A. Mambrin, V. Balduzzi, N. Bernardini, et al., BRAF inhibitors: molecular targeting and immunomodulatory actions, *Cancers* 12 (7) (2020 Jul 7) 1823, <https://doi.org/10.3390/cancers12071823>.
- [12] M. Lang, T. Longerich, C. Anamaterou, Targeted therapy with vemurafenib in BRAF(V600E)-mutated anaplastic thyroid cancer, *Thyroid Res.* 16 (1) (2023 Mar 1) 5, <https://doi.org/10.1186/s13044-023-00147-7>.
- [13] L.A. Dunn, E.J. Sherman, S.S. Baxi, V. Tchekmedyian, R.K. Grewal, S.M. Larson, K.S. Pentlow, S. Haque, R.M. Tuttle, M.M. Sabra, S. Fish, L. Boucai, J. Walters, R.A. Ghossein, V.E. Seshan, A. Ni, D. Li, J.A. Knauf, D.G. Pfister, J.A. Fagin, A.L. Ho, Vemurafenib redifferentiation of BRAF mutant, RAI-refractory thyroid cancers, *J. Clin. Endocrinol. Metab.* 104 (5) (2019 May 1) 1417–1428, <https://doi.org/10.1210/je.2018-01478>.
- [14] Y. Dai, L. Yang, A. Sakandar, D. Zhang, F. Du, X. Zhang, L. Zou, Y. Zhao, J. Wang, Z. Zhang, X. Wu, M. Li, X. Ling, L. Yu, L. Dong, J. Shen, Z. Xiao, Q. Wen, Vemurafenib inhibits immune escape biomarker BCL2A1 by targeting PI3K/AKT signaling pathway to suppress breast cancer, *Front. Oncol.* 12 (2022 Nov 29) 906197, <https://doi.org/10.3389/fonc.2022.906197>.
- [15] B. Ren, H. Liu, Y. Yang, Y. Lian, Effect of BRAF-mediated PI3K/AKT/mTOR pathway on biological characteristics and chemosensitivity of NSCLC A549/DDP cells, *Oncol. Lett.* 22 (2) (2021 Aug) 584, <https://doi.org/10.3892/ol.2021.12845>.
- [16] V. Subbiah, R.J. Kreitman, Z.A. Wainberg, et al., Dabrafenib and trametinib treatment in patients with locally advanced or metastatic BRAF V600-mutant anaplastic thyroid cancer, *J. Clin. Oncol.* 36 (1) (2018 Jan 1) 7–13, <https://doi.org/10.1200/JCO.2017.73.6785>.
- [17] J.T. Wu, C.L. Lin, C.J. Huang, Y.C. Cheng, C.C. Chien, Y.C. Sung, Potential synergistic effects of sorafenib and CP-31398 for treating anaplastic thyroid cancer with p53 mutations, *Oncol. Lett.* 19 (4) (2020 Apr) 3021–3026, <https://doi.org/10.3892/ol.2020.11377>.
- [18] D.M. Hyman, I. Puzanov, V. Subbiah, J.E. Faris, I. Chau, J.Y. Blay, et al., Vemurafenib in multiple nonmelanoma cancers with BRAF V600 mutations, *N. Engl. J. Med.* 373 (8) (2015 Aug 20) 726–736, <https://doi.org/10.1056/NEJMoa1502309>.

- [19] C. Garbe, T.K. Eigentler, Vemurafenib. *Recent Results Cancer Res.* 211 (2018) 77–89, [https://doi.org/10.1007/978-3-319-91442-8\\_6](https://doi.org/10.1007/978-3-319-91442-8_6).
- [20] D. Hanahan, R.A. Weinberg, Hallmarks of cancer: the next generation, *Cell* 144 (5) (2011 Mar 4) 646–674, <https://doi.org/10.1016/j.cell.2011.02.013>.
- [21] Z. Wang, X. Chen, N. Liu, Y. Shi, Y. Liu, L. Ouyang, S. Tam, D. Xiao, S. Liu, F. Wen, Y. Tao, A nuclear long non-coding RNA LINC00618 accelerates ferroptosis in a manner dependent upon apoptosis, *Mol. Ther.* 29 (1) (2021 Jan 6) 263–274, <https://doi.org/10.1016/j.ymthe.2020.09.024>.
- [22] S. Kawanishi, Y. Hiraku, Amplification of anticancer drug-induced DNA damage and apoptosis by DNA-binding compounds, *Curr Med Chem Anticancer Agents* 4 (5) (2004 Sep) 415–419, <https://doi.org/10.2174/1568011043352867>.
- [23] J. Bai, W.B. Chen, X.Y. Zhang, X.N. Kang, L.J. Jin, H. Zhang, Z.Y. Wang, HIF-2 $\alpha$  regulates CD44 to promote cancer stem cell activation in triple-negative breast cancer via PI3K/AKT/mTOR signaling, *World J. Stem Cell.* 12 (1) (2020 Jan 26) 87–99, <https://doi.org/10.4252/wjsc.v12.i1.87>.
- [24] X. Shi, M. Zhu, Z. Gong, T. Yang, R. Yu, J. Wang, Y. Zhang, Homoharringtonine suppresses LoVo cell growth by inhibiting EphB4 and the PI3K/AKT and MAPK/ERK1/2 signaling pathways, *Food Chem. Toxicol.* 136 (2020 Feb) 110960, <https://doi.org/10.1016/j.fct.2019.110960>.
- [25] J. Yang, C. Pi, G. Wang, Inhibition of PI3K/AKT/mTOR pathway by apigenin induces apoptosis and autophagy in hepatocellular carcinoma cells, *Biomed. Pharmacother.* 103 (2018 Jul) 699–707, <https://doi.org/10.1016/j.biopha.2018.04.072>.
- [26] X. Cui, D.W. Qian, S. Jiang, E.X. Shang, Z.H. Zhu, J.A. Duan, *Scutellariae radix* and *coptidis rhizoma* improve glucose and lipid metabolism in T2DM rats via regulation of the metabolic profiling and MAPK/PI3K/AKT signaling pathway, *Int. J. Mol. Sci.* 19 (11) (2018 Nov 18) 3634, <https://doi.org/10.3390/ijms19113634>.
- [27] Z. Qi, S. Kong, S. Zhao, Q. Tang, Naringenin inhibits human breast cancer cells (MDA-MB-231) by inducing programmed cell death, caspase stimulation, G2/M phase cell cycle arrest and suppresses cancer metastasis, *Cell. Mol. Biol.* 67 (2) (2021 Sep 29) 8–13, <https://doi.org/10.14715/cmb/2021.67.2.2>.
- [28] L.P.D.S. Sergio, A.M.C. Thomé, L.A.D.S.N. Trajano, A.L. Menalha, A.S. da Fonseca, F. de Paoli, Photobiomodulation prevents DNA fragmentation of alveolar epithelial cells and alters the mRNA levels of caspase 3 and Bcl-2 genes in acute lung injury, *Photochem. Photobiol. Sci.* 17 (7) (2018 Jul 11) 975–983, <https://doi.org/10.1039/c8pp00109j>.
- [29] Y. Dai, G. Yang, L. Yang, L. Jiang, G. Zheng, S. Pan, C. Zhu, Expression of FOXA1 gene regulates the proliferation and invasion of human gastric cancer cells, *Cell. Mol. Biol.* 67 (2) (2021 Aug 31) 161–165, <https://doi.org/10.14715/cmb/2021.67.2.25>.
- [30] N. Li, F. Yang, D.Y. Liu, J.T. Guo, N. Ge, S.Y. Sun, Scoparone inhibits pancreatic cancer through PI3K/AKT signaling pathway, *World J. Gastrointest. Oncol.* 13 (9) (2021 Sep 15) 1164–1183, <https://doi.org/10.4251/wjgo.v13.i9.1164>.
- [31] X. Chai, J.W. Zhang, S.H. Li, Q.S. Cheng, M.M. Qin, C.Y. Yang, J.L. Gao, H.B. Huang, Xanthoceraside induces cell apoptosis through downregulation of the PI3K/AKT/Bcl-2/Bax signaling pathway in cell lines of human bladder cancer, *Indian J. Pathol. Microbiol.* 64 (2) (2021 Apr-Jun) 294–301, [https://doi.org/10.4103/IJPM.IJPM\\_462\\_19](https://doi.org/10.4103/IJPM.IJPM_462_19).
- [32] G. Deng, L. Ren, M. Wang, et al., DPC4 regulates the proliferation, invasion and epithelial-mesenchymal transition of pancreatic cancer cells by inhibiting PI3K/AKT/mTOR signaling pathway, *Advances in Anatomy* 26 (5) (2020) 567–569+574, [10.16695/j](https://doi.org/10.16695/j.10.16695/j).
- [33] X.F. Liu, J.L. Hao, T. Xie, O.P. Pant, C.B. Lu, C.W. Lu, D.D. Zhou, The BRAF activated non-coding RNA: a pivotal long non-coding RNA in human malignancies, *Cell Prolif.* 51 (2018) e12449, <https://doi.org/10.1111/cpr.12449>.
- [34] Y. Wang, X. Lin, X. Fu, W. Yan, F. Lin, P. Kuang, Y. Luo, E. Lin, X. Hong, G. Wu, Long non-coding RNA BANCR regulates cancer stem cell markers in papillary thyroid cancer via the RAF/MEK/ERK signaling pathway, *Oncol. Rep.* 40 (2) (2018 Aug) 859–866, <https://doi.org/10.3892/or.2018.6502>.
- [35] C. Yao, F. Kong, S. Zhang, G. Wang, P. She, Q. Zhang, Long non-coding RNA BANCR promotes proliferation and migration in oral squamous cell carcinoma via MAPK signaling pathway, *J. Oral Pathol. Med.* 50 (3) (2021 Mar) 308–315, <https://doi.org/10.1111/jop.12968>.